

NDRG1 promotes endothelial dysfunction and hypoxia-induced pulmonary hypertension by targeting TAF15

Chengwei Li[§], Junzhu Lv[§], Gulinuer Wumaier, Yu Zhao, Liang Dong, Yuzhen Zeng, Ning Zhu, Xiujian Zhang, Jing Wang, Jingwen Xia and Shengqing Li*

Department of Pulmonary and Critical Care Medicine, Huashan Hospital, Fudan University, Shanghai 200040, China

*Correspondence: Shengqing Li, shengqing_li@fudan.edu.cn

[§]Chengwei Li and Junzhu Lv contributed equally to this work.

Abstract

Background: Pulmonary hypertension (PH) represents a threatening pathophysiologic state that can be induced by chronic hypoxia and is characterized by extensive vascular remodeling. However, the mechanism underlying hypoxia-induced vascular remodeling is not fully elucidated.

Methods and Results: By using quantitative polymerase chain reactions, western blotting, and immunohistochemistry, we demonstrate that the expression of N-myc downstream regulated gene-1 (NDRG1) is markedly increased in hypoxia-stimulated endothelial cells in a time-dependent manner as well as in human and rat endothelium lesions. To determine the role of NDRG1 in endothelial dysfunction, we performed loss-of-function studies using NDRG1 short hairpin RNAs and NDRG1 over-expression plasmids. *In vitro*, silencing NDRG1 attenuated proliferation, migration, and tube formation of human pulmonary artery endothelial cells (HPAECs) under hypoxia, while NDRG1 over-expression promoted these behaviors of HPAECs. Mechanistically, NDRG1 can directly interact with TATA-box binding protein associated factor 15 (TAF15) and promote its nuclear localization. Knockdown of TAF15 abrogated the effect of NDRG1 on the proliferation, migration and tube formation capacity of HPAECs. Bioinformatics studies found that TAF15 was involved in regulating PI3K-Akt, p53, and hypoxia-inducible factor 1 (HIF-1) signaling pathways, which have been proved to be PH-related pathways. In addition, vascular remodeling and right ventricular hypertrophy induced by hypoxia were markedly alleviated in NDRG1 knock-down rats compared with their wild-type littermates.

Conclusions: Taken together, our results indicate that hypoxia-induced upregulation of NDRG1 contributes to endothelial dysfunction through targeting TAF15, which ultimately contributes to the development of hypoxia-induced PH.

Keywords: N-myc downstream regulated gene-1, TATA-box binding protein associated factor 15, hypoxia-induced pulmonary hypertension, endothelial dysfunction, vascular remodeling

Introduction

Pulmonary hypertension (PH) is a pathophysiological syndrome characterized by an increase in mean pulmonary arterial pressure >20 mmHg at rest,^{1,2} which can complicate the majority of primary diseases.³ Hypoxia-induced PH (HPH), namely group 3 PH, is a type of PH associated with chronic lung diseases.⁴ HPH displays higher morbidity and mortality compared to other PH groups and causes a heavy economic burden globally.⁵⁻⁷ Long-term oxygen therapy can prolong survival but only partially meliorate PH.⁸ The use of approved drugs for group 1 PH has not been shown to benefit patients with HPH in randomized controlled trials.⁹ Hence, a better understanding of disease mechanisms might be helpful in identifying new therapeutic targets for HPH.

The characteristic pathophysiological change in HPH is vascular remodeling induced by hypoxia.¹⁰ PH is a panvasculopathy, meaning that all layers of the vessel wall are involved,¹¹ and each of the resident vascular cell types (i.e. endothelial, smooth muscle, adventitial fibroblast) plays a specific role in the overall remodeling response.¹²⁻¹⁴ Endothelial cells (ECs) form the internal layer

that plays essential roles in sensing the changed oxygen levels; when activated by different factors, like shear hypoxia, the endothelium secretes different growth factors and cytokines to affect EC and smooth muscle cells proliferation, attract inflammatory cells, and/or affect vasoactivity in order to restore homeostasis.¹⁵ As a consequence, the endothelium switches into an overactive state and starts to secrete vasoconstrictive factors,¹⁶ resulting in properties of aberrant proliferation, intimal EC migration, and angiogenesis.¹⁷⁻²⁰ The current treatment is based on the concept of endothelial dysfunction, targeting the endothelin, nitric oxide, and prostacyclin pathways. However, the fundamental disease regulation mechanisms are not addressed. Therefore, these drugs have only resulted in a moderate improvement in morbidity and mortality.²¹

To investigate the molecular mechanism of endothelial dysfunction during hypoxia, we compared pulmonary ECs under normoxia and hypoxia conditions, and identified that N-myc downstream regulated gene-1 (NDRG1) was remarkably upregulated in pulmonary ECs when exposed to hypoxia. NDRG1 belongs to the

Received: July 19, 2023. Accepted: October 7, 2023. Published: 9 October 2023

© The Author(s) 2023. Published by Oxford University Press on behalf of the West China School of Medicine & West China Hospital of Sichuan University. This is an Open Access article distributed under the terms of the Creative Commons Attribution-NonCommercial License

(<https://creativecommons.org/licenses/by-nc/4.0/>), which permits non-commercial re-use, distribution, and reproduction in any medium, provided the original work is properly cited. For commercial re-use, please contact journals.permissions@oup.com

NDRG family containing four members: NDRG1, NDRG2, NDRG3, and NDRG4. NDRG1 plays multifunctional roles in cell growth, development, differentiation, and stress responses.^{22,23} However, whether NDRG1 associates with endothelial dysfunction during hypoxia and whether it plays a role in vascular remodeling have largely not been elucidated. NDRG1 is expressed widely in human tissues, but is hardly detectable in normal ECs,²⁴ suggesting that hypoxia might specifically upregulate NDRG1 in these cells and then facilitate hypoxia-induced PH.

In this study, we demonstrated that the expression of NDRG1 was markedly increased in hypoxia-stimulated ECs in a time-dependent manner and in human and rat endothelium lesions. We revealed the potential function of NDRG1 in endothelial dysfunction and vascular remodeling *in vivo* and *in vitro*, and then explored its underlying mechanisms. Our results disclose a critical role of NDRG1 in the pathogenesis of HPH.

Materials and methods

Pulmonary surgical specimens

The study was approved by the local ethical committee (KY2016-396), and written informed consent was obtained from all patients for donated lung tissues. Surgical specimens of lung tissue were collected from patients with chronic lung disease-associated PH ($n = 3$) or corresponding non-tumor normal tissues without PH ($n = 3$). Demographic information of the recruited PH patients and donor controls is provided in the supplementary materials available online.

Animal models and *in vivo* gene knockdown

Adult male Sprague-Dawley rats weighing 150–200 g were purchased from the Shanghai SLAC Laboratory Animal Co. Ltd (Shanghai, China). All protocols and surgical procedures were approved by the Ethics Committee of Experimental Research at Fudan University Shanghai Medical College (202210016S) and conducted in the Shanghai Medical College. All animals were housed under a 12:12 h light/dark cycle and had free access to sterile food and water. The room temperature was controlled at $22 \pm 1^\circ\text{C}$ and relative humidity was maintained at $50\% \pm 5\%$. A rat HPH model was established based on a previous study.^{25,26} Briefly, animals were divided randomly into the following two groups: (i) normoxia and (ii) chronic hypoxia. Rats in the normoxia group were housed at ambient barometric pressure for 28 days (~ 718 mmHg, $\text{PO}_2 \sim 150.6$ mmHg). Rats in the hypoxia groups were housed in a hypobaric hypoxia chamber depressurized to 380 mmHg (PO_2 was reduced to ~ 79.6 mmHg) for 8 h/day for 28 days.

Short hairpin RNA (shRNA) against rat NDRG1 and a negative control shRNA were designed and synthesized by GenScript, China. Entranster *in vivo* transfection reagent (Engreen Biosystem, China) was used as a vehicle for shRNA delivery according to the manufacturer's recommendations. The shRNAs against NDRG1 or negative control (1 mg/kg) was injected into the tail veins of SD rats once per week during normoxia or hypoxia treatment.

Echocardiography

Echocardiography was performed under anesthesia (2% isoflurane mixed with air), with the Vevo3100 Ultrasound system (GE Healthcare) and the 12S rodent probe (GE Healthcare) to determine pulmonary artery acceleration time (PAAT, in pulsed wave Doppler mode; eight to ten measurements performed for each rat), tricuspid annular plane systolic excursion (TAPSE), and heart rate. Data were analyzed with EchoPAC software (GE Healthcare).

Measurement of haemodynamics and tissue preparation

Rats were anesthetized with 2% sodium pentobarbital (50 mg/kg i.p.) after exposure to hypoxia for 28 days. Then, the right ventricular systolic pressure (RVSP) was measured through right jugular vein puncture to the right ventricle (RV) with a transducer and was recorded by the PowerLab system (AD Instruments, Australia). Following euthanasia, both the rat lungs and hearts were collected. The weights of the RVs and left ventricle plus septum (LV + S) were measured separately, and the RV/LV + S weight ratio was determined to indicate right ventricular hypertrophy. Next, the lower lung lobes were sectioned into 4-mm-thick slices and soaked in a 10% formalin solution (pH = 7.4). The other tissues were kept in liquid nitrogen for further experiments.

Hematoxylin and eosin staining

The lung lobes were sliced and embedded in paraffin, and cut into $\sim 5\text{-}\mu\text{m}$ -thick sections using a microtome. Then, the sections were placed on glass slides, stained with hematoxylin and eosin (H&E) for morphological analysis, and visualized under an Olympus microscope (Tokyo, Japan). The medial wall thickness was analyzed with ImageJ software (National Institutes of Health, USA) and is expressed as the ratio of medial area to cross sectional area (medial/CSA).

Immunohistochemical analysis

Paraffin-embedded tissues were cut into $4\text{-}\mu\text{m}$ -thick sections, and tissue sections were deparaffinized in xylene and rehydrated in alcohol. Sections were heated for 5 min in a pressure cooker to repair antigenicity, treated with 3% H_2O_2 to inactivate endogenous peroxidase activity for 10 min, and incubated with goat serum for 10 min to block nonspecific antibody binding. Sections were incubated with the mouse anti-NDRG1 monoclonal antibody (1/200, Santa Cruz, CA) overnight at 4°C . After incubation with the secondary antibody, the signal was developed with 3,3'-diaminobenzidine.

Cell culture

Human pulmonary arterial endothelial cells (HPAECs) (ScienCell Research Laboratories, USA) were cultured according to the manufacturer's instructions. HPAECs (5–8 passages) were cultured in complete endothelial cell medium (ECM) with 5% fetal bovine serum (FBS) and 1% penicillin-streptomycin solution. Cells were used for experiments at 80%–90% confluence. Cells in the normoxia group were maintained at 37°C in 21% O_2 and 5% CO_2 (Thermo Fisher Scientific, USA). Cells in the hypoxia groups were cultured at 37°C in 1% oxygen, 94% N_2 , and 5% CO_2 (Thermo Fisher Scientific, USA).

Establishment of stable cell clones

Lentiviral vectors for shRNAs targeting NDRG1 or TATA-box binding protein associated factor 15 (TAF15) and the lentiviral pCDH vector for NDRG1 overexpression were purchased from Addgene (Cambridge, MA, USA). These vectors together with the packaging vectors (Addgene) were transfected into HEK293T cells for preparation of recombinant lentiviruses. HPAECs were infected by lentiviruses in the presence of polybrene (5 $\mu\text{g}/\text{ml}$). Cells were selected for 1 week using puromycin (2 $\mu\text{g}/\text{ml}$) after infection for 72 h. The selected cell lines were prepared for subsequent experiments.

Proliferation assay

Proliferation of HPAECs was measured using a 5-ethynyl-20-deoxyuridine (EDU) incorporation assay kit (C0075S, Beyotime Biotechnology) and Cell Counting Kit-8 (CCK-8) assay (C0041, Beyotime Biotechnology), according to the manufacturer's instructions. For the EDU assay, the HPAECs were seeded into 24-well plates at 1×10^5 cells/well and incubated for 24 h under different conditions. Cells were washed with phosphate buffered saline (PBS) for 5 min twice before incubation with 4% paraformaldehyde for 30 min. After washing with PBS for 5 min twice, samples were permeated with 0.3% TritonX-100 in PBS and dyed with reaction solution. Images were taken under a laser scanning confocal microscope (Olympus, Japan) and the percentage of red (EDU) to blue (Hoechst) cells was calculated. For the CCK-8 assay, the HPAECs were seeded into 96-well plates at 5×10^3 cells/well in complete medium under normoxic conditions. Cells were treated under different conditions and then the culture medium was removed. A total of 110 μ l of ECM containing CCK-8 [CCK-8 : ECM (v/v) = 1 : 10] was added to each well and the cells were incubated for 4 h. Finally, absorbance at 450 nm was measured using an Epoch Microplate Spectrophotometer (BioTek, USA).

EC migration

A 24-well transwell plate (8 μ m pore size, Corning, USA) was used to measure cell migration. A total of 1×10^4 cells in 250 μ l of serum-free ECM were placed into the upper chamber and 500 μ l of ECM containing 10% FBS was added to the lower chambers. Then the plates were placed in different conditions for 24 h. Cells on the top side of each insert were then scraped off and the wells were fixed in 4% paraformaldehyde, stained by crystal violet, photographed, and counted under a microscope (Olympus, Japan).

EC tube formation assays

Precooled 48-well plates were coated with 150 μ l of Matrigel (#354 248, Corning, USA) at 37°C for 30 min. The HPAECs treated under different conditions were seeded at 1×10^4 cells/well and cultured for 6–8 h. Tube formation was observed under a microscope (Olympus, Japan) and the tube lengths were calculated using Image J software (National Institutes of Health, USA).

Immunofluorescence staining

The HPAECs treated under different conditions were fixed with 4% paraformaldehyde, permeabilized with 0.5% Triton X-100, blocked with donkey serum, and incubated with primary antibodies against NDRG1 (#sc-398291) or TAF15 (#CST28409) at 4°C overnight, followed by incubation with Alexa Fluor-conjugated secondary antibodies (Jackson ImmunoResearch, USA) for 2 h at 37°C. Cells were then counterstained with 4,6-diamidino-2-phenylindole (DAPI). Staining was visualized and photographed via a laser scanning confocal microscope (Olympus, Japan).

Quantitative real-time PCR

Total RNA was extracted using Trizol reagents (Invitrogen, USA) from lung tissue or cultured HPAECs. Reverse transcription was performed using HiScript II SuperMix reverse transcriptase (Vazyme). cDNA was amplified and detected using Hieff qPCR SYBR Green Master Mix (YEASEN, China). The relative expression level of mRNA was calculated by the $2^{-\Delta\Delta CT}$ method. The quantitative real-time (qRT)-PCR primers were designed and synthesized by Sunny Biotechnology (Shanghai, China), and

the primer sequences are shown in the online supplementary materials.

Nuclear and cytoplasmic protein extraction

Cell pellets were prepared and treated according to the instructions of a nuclear and cytoplasmic protein extraction kit (Beyotime Biotechnology, China) to isolate nuclear proteins from the cytoplasm. The proteins extracted were assessed by western blotting. β -Actin (Proteintech) and histone-H3 (CST) were used as loading controls for cytosolic and nuclear proteins, respectively.

Liquid chromatography mass spectrometry analysis

To investigate the potential proteins binding to NDRG1, a total of 500 μ g of cell lysate was extracted from HPAECs with Nonidet P 40 (NP-40) buffer and then centrifuged at 12 000 \times g at 4°C for 30 min to remove cell debris. Five percent of the cell lysates were kept as inputs. The rest was precleared with Protein G Magnetic Beads (Bio-Rad, USA) for 2 h at 4°C and then immunoprecipitated with the corresponding antibodies overnight at 4°C. The beads were harvested, and the bound proteins were then separated by 10% sodium dodecyl sulphate-polyacrylamide gel electrophoresis (SDS-PAGE) and stained with mass silver stain (Sangon Biotech Shanghai Co., Ltd.). The proteins were extracted from the gel, re-suspended in 100 μ l of double distilled water (ddH₂O), and analyzed by mass spectrometry via high-performance liquid chromatography and a Q Exactive Mass Spectrometer (Thermo Scientific, Waltham, MA, USA) at the Shanghai Applied Protein Technology Co., Ltd. The original files were transformed with Proteomics Tools 3.1.6 software, and Mascot 2.2 software was used for database screening.

Coimmunoprecipitation and immunoblotting

Cells were lysed in NP-40 buffer (1 mM Phenylmethylsulfonyl Fluoride) for 1 h on ice, and were then centrifuged at 12 000 \times g at 4°C for 30 min to remove cell debris. Five percent of the cell lysates were kept as inputs. The rest was precleared with Protein G Magnetic Beads (Bio-Rad, USA) for 2 h at 4°C and then immunoprecipitated with the corresponding antibodies overnight at 4°C. The beads were harvested, and the bound proteins were resolved by SDS-PAGE and analyzed by western blotting. For western blotting, cells were lysed in Radio Immunoprecipitation Assay (RIPA) buffer for 1 h on ice and centrifuged at 12 000 \times g at 4°C for 30 min to remove cell debris. Protein samples were subjected to SDS-PAGE and transferred onto polyvinylidene fluoride membranes, followed by blocking and probing with the indicated antibodies for detection. Incubation with appropriate secondary antibodies (Jackson Immuno Research Laboratories, USA) was also performed. A chemiluminescence ECL kit (Yeasen, China) was used to detect the protein bands of interest and band density was quantified by Image J software (National Institutes of Health, USA). The antibodies used for immunoprecipitation (IP) and the primary antibodies for western blotting were as follows: NDRG1 (1 : 5000, Abcam, ab124689), TAF15 (1 : 1000, #CST28409), β -actin (1 : 8000, #66009-1-Ig, ProteinTech, USA), histone-H3 (1 : 2000, #4499, CST), and α -tubulin (1 : 8000, # Abmart T40103).

Bioinformatics analysis

Raw gene expression data GSE11341 were downloaded from the Gene Expression Omnibus (GEO) (<http://www.ncbi.nlm.nih.gov/geo/>) of the National Center for Biotechnology Information (NCBI).

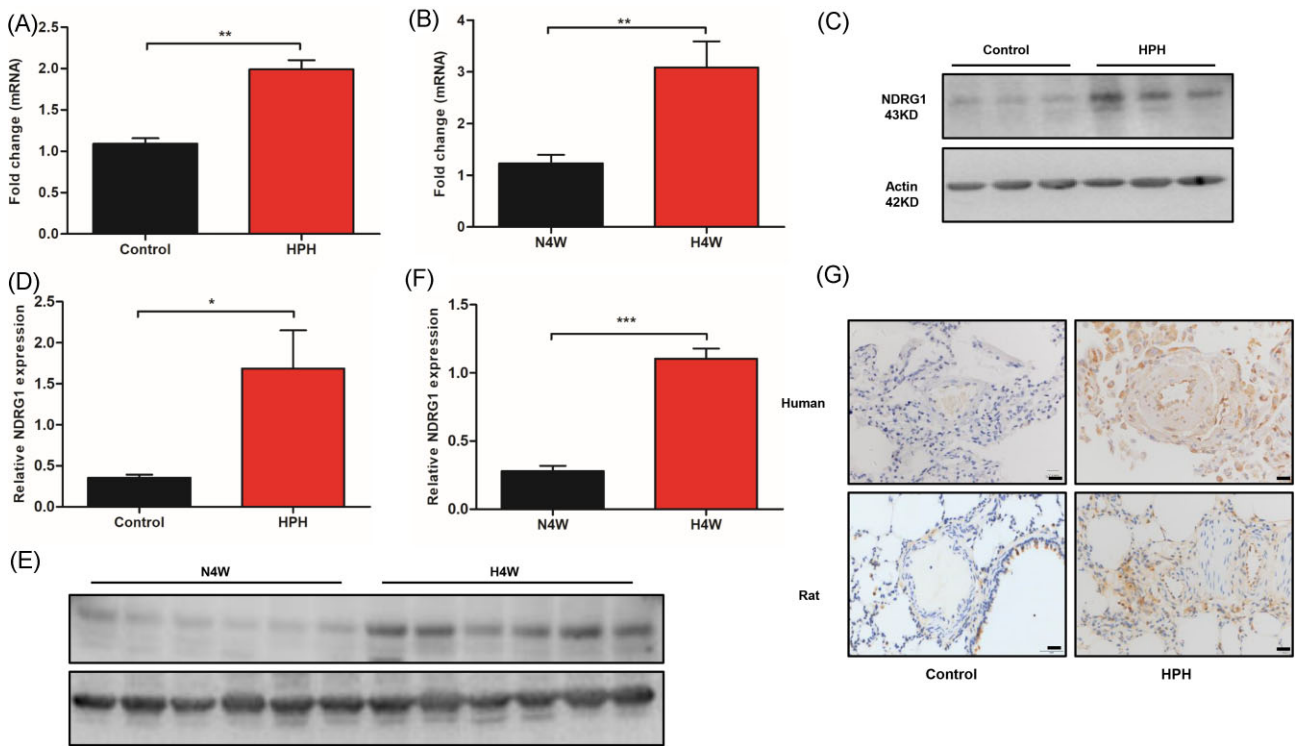


Figure 2. NDRG1 is highly expressed in pulmonary vessels of patients with HPH and HPH model rats. (A) Expression of NDRG1 in lung homogenates of HPH measured by qRT-PCR; data are presented as fold-change relative to donors ($n = 3$, respectively). (B) Expression of NDRG1 in lung homogenates of HPH model rats measured by qRT-PCR; data are presented as fold-change relative to the control group ($n = 6$, respectively). (C) Expression of NDRG1 in lung homogenates of HPH determined by western blot and quantitated by densitometric analysis (D). (E) Expression of NDRG1 in lung homogenates of HPH model rats determined by western blot and quantitated by densitometric analysis (F). (G) IHC showing expression of NDRG1 in the tissues from normal subjects and patients with HPH (upper panels), or from control and HPH model rats (lower panels). Scale bar, $20 \mu\text{m}$. * $P < 0.05$, ** $P < 0.01$, *** $P < 0.001$ versus donors.

results revealed that NDRG1 expression is induced by hypoxic exposure time-dependently in HPAECs.

NDRG1 expression is markedly upregulated in HPH lung samples

To investigate the involvement of NDRG1 in the progression from normal lung to HPH, we firstly measured NDRG1 mRNA expression in representative human lung samples from normal individuals and patients with HPH, as well as normoxia rats and hypoxia-treated rats. In contrast to control donors, NDRG1 was significantly upregulated in the lung of patients and hypoxia-treated rats at mRNA level (Fig. 2A and B). In line with our findings at mRNA level, NDRG1 protein expression significantly increased in the lung of patients and hypoxia-treated rats compared with those of controls (Fig. 2C–F). To further confirm this result, we performed immunohistochemistry (IHC) staining in the same tissue sample section. The IHC results showed that a strong immunoreactivity of NDRG1 was observed in the intimal layer of pulmonary arteries of subjects with HPH compared with those from normal donors ($n = 3$ for each), as well as in those of HPH model rats when compared with normal rats ($n = 6$ for each) (Fig. 2G, supplementary Fig. S1, see online supplementary material). These data suggest that NDRG1 might play a regulatory role in the pathogenesis of HPH.

Effect of NDRG1 knockdown and overexpression on proliferation, migration, and angiogenic response of HPAECs

To explore the role of NDRG1 in endothelial dysfunction, we firstly knocked down endogenous NDRG1 in HPAECs

through infection with lentiviruses containing three specific shRNAs (supplementary Fig. S2, A–D, see online supplementary material). The desired gene knockdown was achieved in hypoxia-exposed cells after expression of NDRG1-targeted (NDRG1-KD2 and NDRG1-KD3) but not control (NDRG1-NC) shRNAs (supplementary Figure S2B–D). We next evaluated the effects of NDRG1 silencing on the proliferation of HPAECs via EDU and CCK-8 assays. The results showed that NDRG1 knockdown decreased the ratios of EDU-positive HPAECs and the viability of cells (Fig. 3A–C). Transwell assays showed that it also reduced the migration of HPAECs (Fig. 3D and E). Finally, tube formation assays were performed to evaluate the effect of NDRG1 deficiency on angiogenesis. As a result, NDRG1 knockdown significantly reduced branching and tubule length of HPAECs (Fig. 3F–H). We next examined the effect of NDRG1 overexpression on proliferation, migration, and angiogenic response of HPAECs. Abundant gene expression was observed after lentivirus-based delivery of NDRG1 (supplementary Figure S3A–D, see online supplementary material). NDRG1 overexpression led to a substantial increase in proliferation (Fig. 4A–C), migration (Fig. 4D and E) and angiogenic response of HPAECs (Fig. 4F–H). Taken together, these results clearly demonstrated that NDRG1 promotes the proliferation, invasion, and tube formation of HPAECs.

NDRG1 directly interacts with TAF15 and regulates the subcellular localization of TAF15

To further explore the regulatory network of NDRG1, we performed an IP assay to identify its potential interacting partners. Further mass spectrometry analysis (IP-MS) indicated that TAF15,

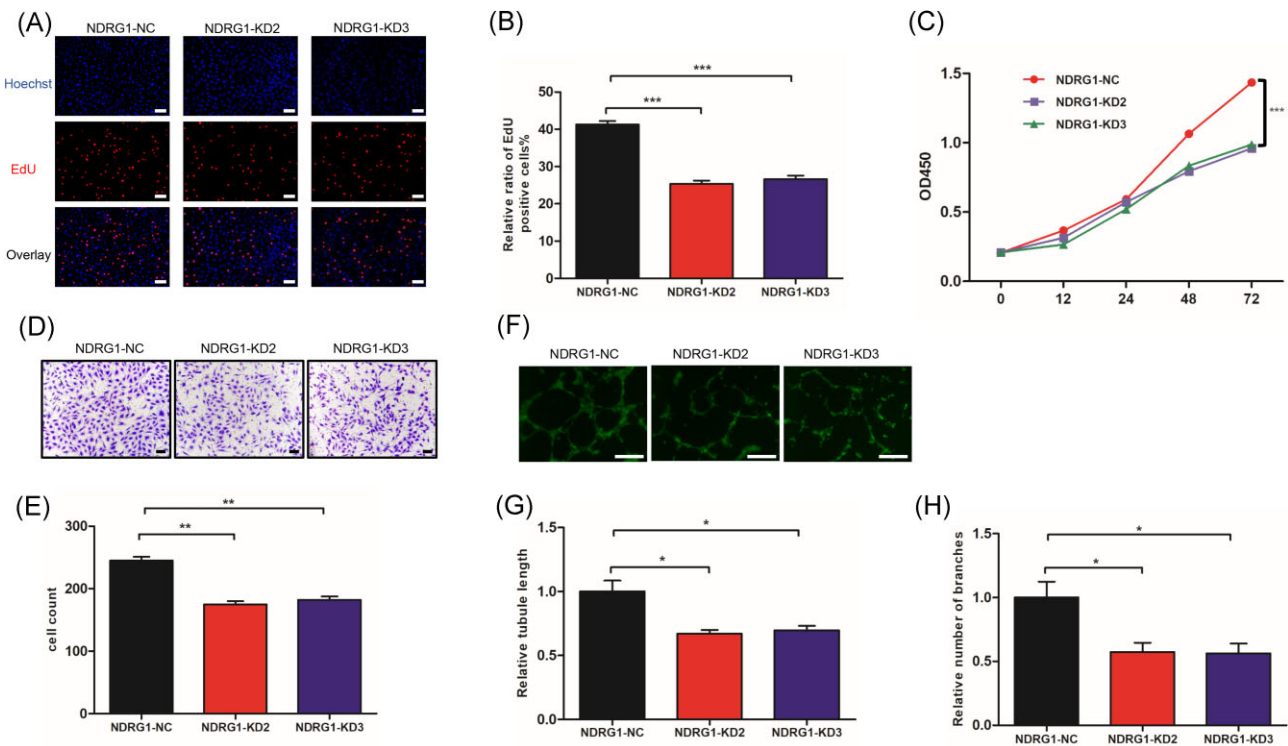


Figure 3. NDRG1 knockdown inhibits the proliferation, migration, and angiogenic response of HPAECs under hypoxia. **(A)** HPAEC proliferation was measured by EDU assay in control (NDRG1-NC) and NDRG1 knockdown (NDRG1-KD2 and NDRG1-KD3) cells followed by hypoxia exposure. Scale bar, 100 μ m. **(B)** Ratios of red (EDU) to blue (Hoechst) cells were plotted. **(C)** Control and NDRG1 knockdown HPAECs were exposed to hypoxia for the indicated times (hours on the x-axis) and subjected to CCK-8 assay. **(D)** Control and NDRG1 knockdown HPAECs were exposed to hypoxia for 24 h and cell migration was measured by transwell assay. Scale bar, 200 μ m. **(E)** Cells migrating to the lower chambers were counted. **(F)** Control and NDRG1 knockdown HPAECs were exposed to hypoxia for 6–8 h and the angiogenic response was measured by tube formation. Scale bar, 200 μ m. The results are shown as relative length of tubules **(G)** and relative number of branches **(H)** formed by HPAECs. * $P < 0.05$, ** $P < 0.01$, *** $P < 0.001$.

a component of RNA polymerase II, was among the candidate proteins binding to NDRG1 (Fig. 5A). We further confirmed the direct binding of TAF15 with NDRG1 via IP analysis. As expected, NDRG1 efficiently co-immunoprecipitated with TAF15 in HPAECs (Fig. 5B). Immunofluorescence staining results showed that NDRG1 co-localized with TAF15 in the nuclei of HPAECs (Fig. 5C–E). Since NDRG1 knockdown or overexpression failed to affect the protein levels of TAF15 (supplementary Figure S4A and B, see online supplementary material), we explored whether the subcellular localization of TAF15 was regulated by NDRG1. Indeed, western blot analysis of separated nuclear and cytoplasmic proteins showed that the levels of TAF15 decreased in the nucleus after NDRG1 knockdown, while NDRG1 overexpression promoted the nuclear localization of TAF15 (Fig. 5F–I). On the other hand, the levels of TAF15 increased in the cytoplasm after NDRG1 knockdown, while NDRG1 overexpression decreased the cytoplasm localization of TAF15 (supplementary Figure S5A and B, see online supplementary material). Regulation of the subcellular localization of TAF15 by NDRG1 was further verified by immunofluorescence staining (Fig. 5K and L). Thus, NDRG1 binding facilitates nuclear accumulation of TAF15 in hypoxic HPAECs.

NDRG1 regulates endothelial dysfunction through TAF15

To the best of our knowledge, our results demonstrated that TAF15 is a new interaction protein of NDRG1. To validate whether TAF15 is necessary for NDRG1 to regulate endothelial dysfunction, we knocked down TAF15 in HPAECs (supplementary Figure S6A and B, see online supplementary material) and performed

EDU and CCK-8 assays, transwell assays, and tube formation assays. We observed that TAF15 silencing counteracted the proliferation (Fig. 6A–C) and migration (Fig. 6D and E) of HPAECs induced by NDRG1 overexpression. TAF15 knockdown also abrogated the effect of NDRG1 on *in vitro* tube formation of HPAECs, as evidenced by reduced branches and tubule length of HPAECs (Fig. 6F–H). Taken together, these results indicated that NDRG1 causes endothelial dysfunction through inducing nuclear translocation and activation of TAF15. To further explore the downstream signalling pathway of TAF15 in HPAECs, we silenced TAF15 and performed RNA-seq to screen for DEGs. The DEGs were then analyzed by GO and KEGG pathway enrichment analysis (supplementary Fig. S7, see online supplementary material). GO analysis showed that TAF15 may be involved in the regulation of cell migration, angiogenesis, and proliferation (Fig. 6I). KEGG pathway enrichment analysis of DEGs showed significant association of TAF15 with PI3K-Akt, p53, and hypoxia-inducible factor 1 (HIF-1) signalling pathways (Fig. 6J). Therefore, TAF15 activation is likely to impair endothelial homeostasis through regulation of classic pathways related to PH.

Knockdown of NDRG1 alleviates hypoxia-induced vascular remodeling and right ventricular hypertrophy

To further validate its role in hypoxia-induced PH, we knocked down NDRG1 in normoxia (N4W) or chronic hypoxia (H4W) exposed rats via *i.v.* administration of the shRNAs (supplementary Figure S8A and B, see online supplementary material). Echo-Doppler scans showed greater PAATs (Fig. 7A and C) and a smaller

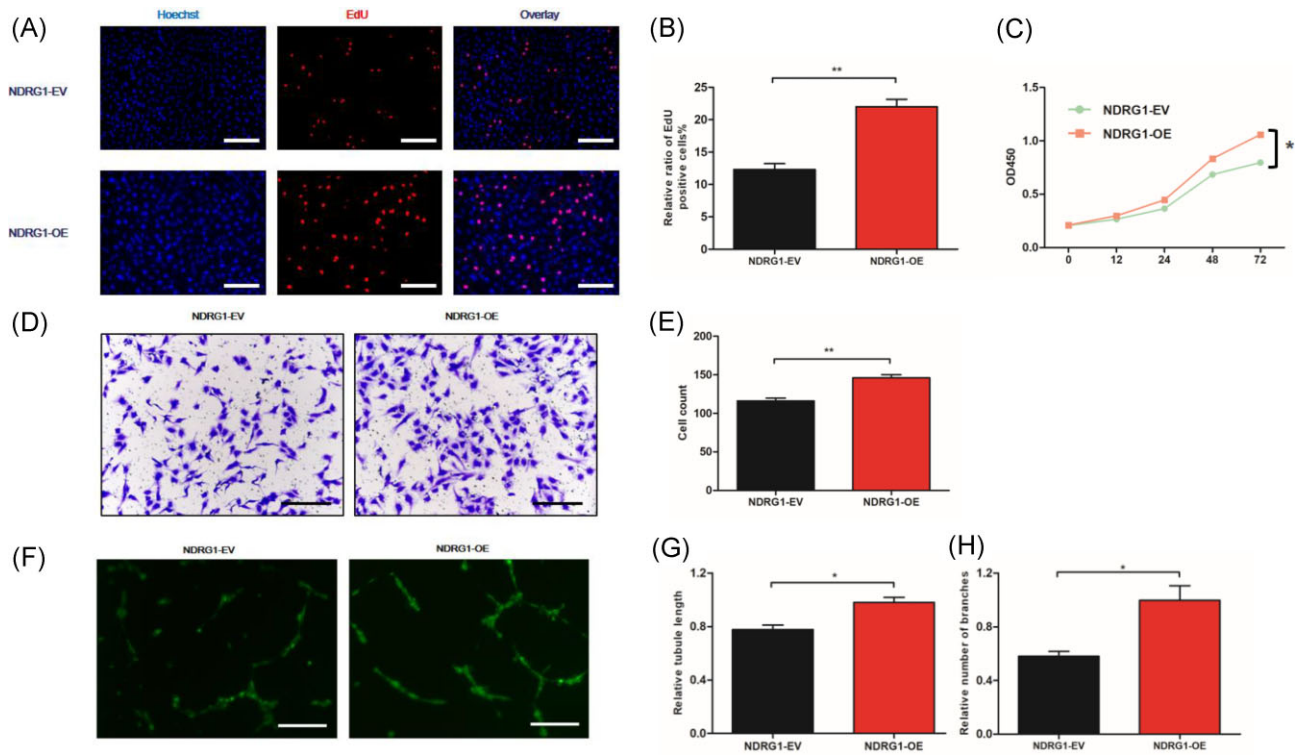


Figure 4. NDRG1 overexpression promotes proliferation, migration, and angiogenic response of HPAECs. **(A)** HPAEC proliferation was measured by EDU assay in control (NDRG1-EV) and NDRG1 overexpression (NDRG1-OE) cells. Scale bar, 100 μm . **(B)** Ratios of red (EDU) to blue (Hoechst) cells were plotted. **(C)** Control and NDRG1-OE HPAECs were exposed to normoxia for the indicated times (hours on the x-axis) and subjected to CCK-8 assay. **(D)** Control and NDRG1-OE HPAECs were exposed to normoxia for 24 h and cell migration was measured by transwell assay. Scale bar, 200 μm . **(E)** Cells migrating to the lower chambers were counted. **(F)** Control and NDRG1-OE HPAECs were exposed to normoxia for 6–8 h and the angiogenic response was measured by tube formation. Scale bar, 200 μm . The results are shown as relative length of tubules **(G)** and relative number of branches **(H)** formed by HPAECs. * $P < 0.05$, ** $P < 0.01$.

TAPSEs (Fig. 7B and D) in hypoxia-exposed rats subjected to NDRG1 knockdown than in those injected with a control shRNA, although no difference was observed between control and NDRG1 knockdown groups in rats raised in normoxic conditions. As shown in Fig. 7E and F, knockdown of NDRG1 markedly attenuated hypoxia-induced PH and right ventricular hypertrophy as measured by RVSP and RV/LV + S weight ratio. Consistently, hypoxia induced $<100 \mu\text{m}$ intrapulmonary arteriole remodeling, while NDRG1 knockdown alleviated hypoxia-induced pulmonary vascular remodeling, as evidenced by decreased pulmonary vascular wall thickness and muscularization, and the ratio of medial area to CSA (medial/CSA) (Fig. 7G–I). These results confirmed the promoting role of NDRG1 in the pathogenesis of HPH by regulating haemodynamic changes and pulmonary vascular remodeling.

Discussion

In the present study, we demonstrate that the expression of NDRG1 is markedly upregulated in hypoxia-stimulated HPAECs as well as in the endothelium of pulmonary arteries from patients and HPH model rats. Specific knockdown of NDRG1 expression in HPAECs substantially inhibits the dysfunction such as proliferation, migration, and angiogenic response in HPAECs. Furthermore, we found that shRNA-mediated knockdown of NDRG1 attenuates the hypoxia-induced elevation of RVSP, right ventricular hypertrophy, and medial wall thickness of muscularized distal pulmonary arterioles in rats. Mechanistically, we found that NDRG1 functionally interacts with TAF15 and promotes its nuclear localization. Bioinformatics study showed that TAF15 was involved in regulat-

ing PI3K-Akt, p53, and HIF-1 signaling pathways, which have been proved to be PH-related pathways. Taken together, our results indicate that hypoxia-induced up-regulation of NDRG1 contributes to endothelial dysfunction through targeting TAF15, which ultimately contributes to the development of HPH.

Omics technology holds great promise to identify new biomarkers and thereby improve the diagnosis and treatment of PH.²⁸ In this study, we searched a GEO dataset (GSE11341),²⁷ and found that NDRG1, known to be absent in normal ECs, was highly expressed in ECs stimulated by hypoxia, indicating that NDRG1 may be involved in the response to acute and chronic hypoxia in ECs. As a gene related to hypoxia stress, NDRG1 could be transcriptionally activated by HIF-1 α and ETS proto-oncogene 1 (ETS1).²⁹ HIF-1 was reported to drive the initial response to acute hypoxia (2–24 h) and HIF-2 is a key player in the chronic response (48–72 h).³⁰ Our study found that NDRG1 is still highly expressed after hypoxia exposure for 24 h, with a similar trend to HIF-2 α expression at protein level (data not shown), suggesting that NDRG1 may be regulated by both HIF-1 α and HIF-2 α . Nonetheless, further studies are required to determine how NDRG1 is upregulated in HPAECs during the pathogenesis of HPH.

The involvement of NDRG1 in HPH was demonstrated by our studies, which showed that NDRG1 was markedly upregulated in the pulmonary vasculatures of both patients and rats with HPH. Consistent with our study, Grigoryev *et al.* identified elevated *NdrG1* in lung tissue of 10 h hypoxic mice.³¹ Hu *et al.* first established that pulmonary arteries from human and bovine PH lungs exhibit markedly increased

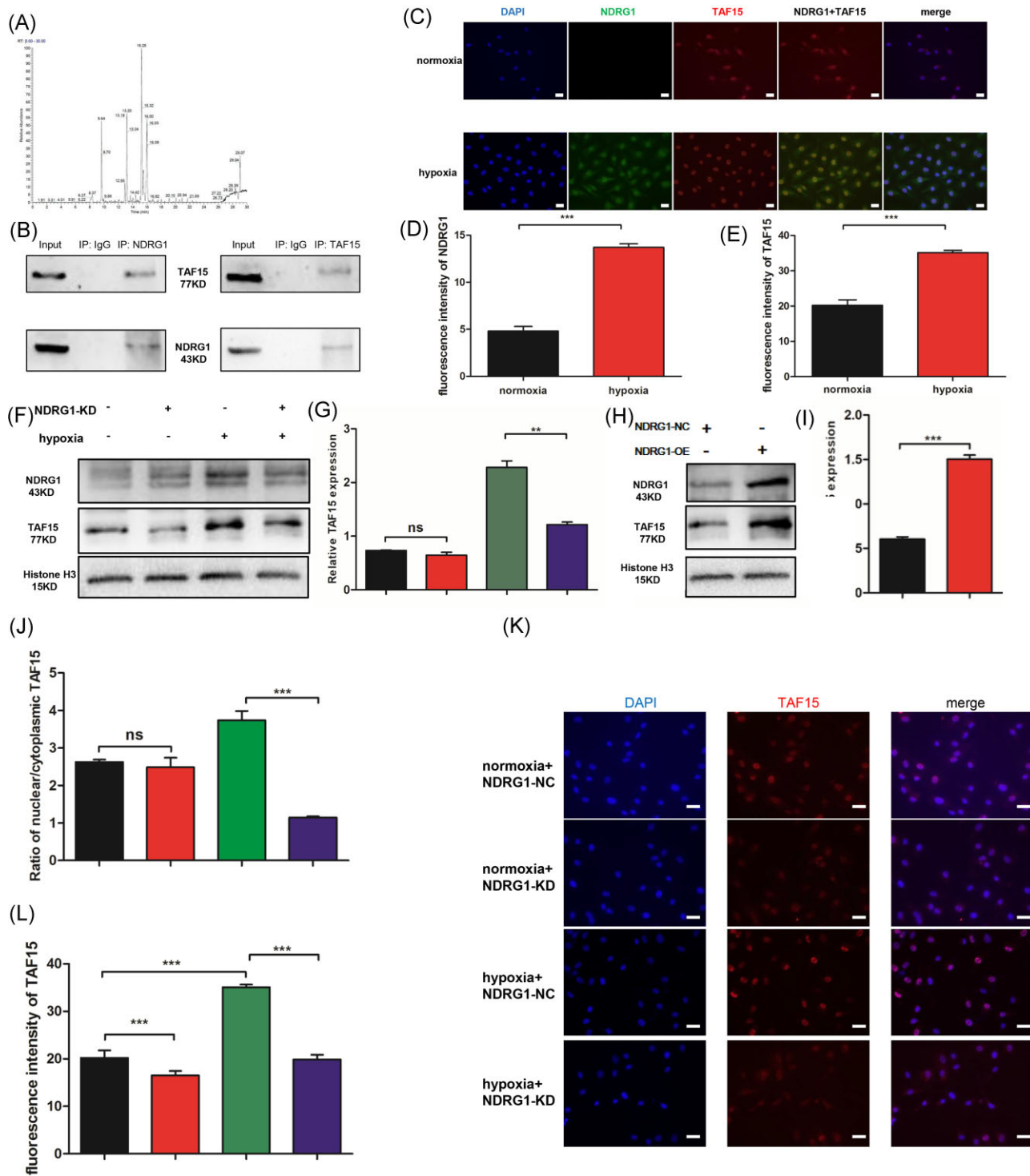


Figure 5. NDRG1 interacts with TAF15 and regulates the subcellular localization of TAF15 in HPAECs. **(A)** The lysates of HPAECs were immunoprecipitated with an NDRG1 antibody, and mass spectrometry analysis was conducted to discover the potential interacting protein. Trypsin-digested fragment detected by mass spectrometry is presented. **(B)** Lysates of HPAECs were subjected to IP and subsequent immunoblotting with the indicated antibodies. **(C)** HPAECs were exposed to normoxia or hypoxia for the indicated times, and were subjected to immunofluorescence staining for NDRG1 (green) and TAF15 (red). The nuclei of cells were counterstained with DAPI (blue). Scale bar, 20 μ m. The fluorescence intensity of NDRG1 **(D)** and TAF15 **(E)** immunostaining in the nucleus were measured and statistically analyzed. HPAECs were subjected to hypoxia exposure and/or knockdown of NDRG1, followed by preparation of nuclear extracts of cells. Western blot analysis of the nuclei for NDRG1 knockdown **(F)** and NDRG1 overexpression **(H)** of HPAECs proteins was then performed. Histone H3 was blotted as the loading control for the nuclear proteins **(G, I)**. **(J)** Ratio of nuclear/cytoplasmic TAF15 was measured and statistically analyzed. **(K)** HPAECs were treated as described in **(A)**, and were subjected to immunofluorescence staining for NDRG1 (green) and TAF15 (red). The nuclei of cells were counterstained with DAPI (blue). Scale bar, 20 μ m. **(L)** The fluorescence intensity of TAF15 immunostaining in the nucleus was measured and statistically analyzed. ** $P < 0.01$, *** $P < 0.001$; ns, not significant.

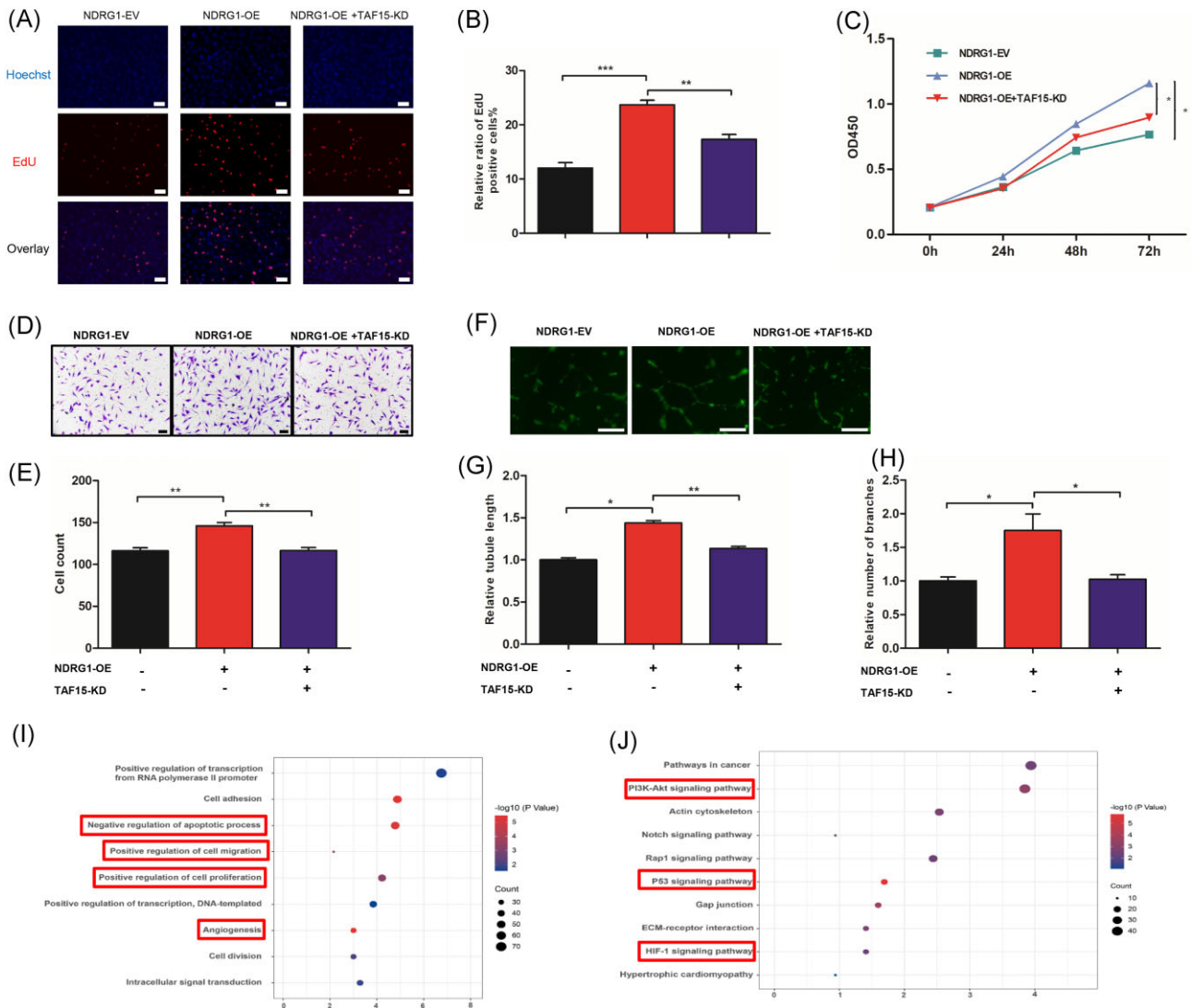


Figure 6. NDRG1 regulates HPH-related phenotypes of HPAECs through TAF15. **(A)** HPAECs were transfected with control or NDRG1-overexpressing (OE) constructs, and with TAF15-targeted shRNAs (TAF15-KD), and cell proliferation was measured by EDU assay 24 h after transfection. Scale bar, 100 μ m. **(B)** The ratios of red (EdU) to blue (Hoechst) cells were plotted. Scale bar, 100 μ m. **(C)** Cells were transfected as described in **(A)** and were subjected to CCK-8 assay. HPAECs were transfected as described in **(A)**, and were subjected to measurement for migration by transwell assay **(D, E)** and angiogenic response by tube formation **(F-H)**. Scale bar in **(D)** and **(F)**, 200 μ m. * $P < 0.05$, ** $P < 0.01$, *** $P < 0.001$. The DEGs were then analyzed by **(I)** BP and **(J)** KEGG pathway enrichment analysis.

expression of direct HIF target genes, including NDRG1.³² Additionally, we observed that increased NDRG1 expression occurred in the endothelium of HPH vessels compared to donor vessels, suggesting that NDRG1 might be involved in endothelial dysfunction. Hence, further study confirmed that NDRG1 positively regulates the proliferation, migration, and angiogenic response of HPAECs. NDRG1 plays multifunctional roles in cell growth, development, differentiation, and stress response of various cells including ECs.^{22,23} Knockdown of NDRG1 decreased hemangioma EC proliferation and downregulated the c-MYC oncoprotein.³³ Ablation of NDRG1 attenuated endothelial inflammation, thrombotic responses, and vascular remodeling.³⁴ Repression of NDRG1 decreased migration of ECs and impaired neoangiogenesis under intermittent hypoxia conditions.³⁵ In addition, NDRG1 deficiency in ECs prevented aorta angiogenesis and the activation of phospholipase C γ 1 (PLC γ 1) and extracellular regulated protein kinases (ERK)1/2 by vascular endothelial growth factor (VEGF)-A.³⁶ To ascertain the inherent effect of NDRG1 in the progression of PH,

we used an *in vivo* model of knockdown of NDRG1 in HPH rats. As shown by multiple detection methods, knockdown of NDRG1 significantly prevented the progression of hypoxia-induced PH and right ventricular hypertrophy, as demonstrated by the decreased RVSP and RV/LV + S weight ratio. Consistent with hemodynamics, histopathology proved that NDRG1 knockdown alleviated hypoxia-induced pulmonary vascular remodeling, as evidenced by decreased pulmonary vascular wall thickness and muscularization, and medial/CSA ratio. Consistent with our study, another research reported that adeno-associated virus (AAV)-mediated NDRG1 silencing played a protective role in hypoxia-induced pulmonary hypertension via dynamin-related protein (DRP)1 and PI3K/Akt/mTOR signaling pathways in pulmonary artery smooth muscle cells.³⁷ Hypoxia inhibits testis-expressed 261 (Tex261), a protein-coding gene, to promote hPASMC proliferation through NdrG1-Akt-induced Sec23 downregulation.³⁸ Interestingly, digoxin, an inhibitor of Na⁺/K⁺ ATPase, has also been reported to downregulate NDRG1 through the inhibition

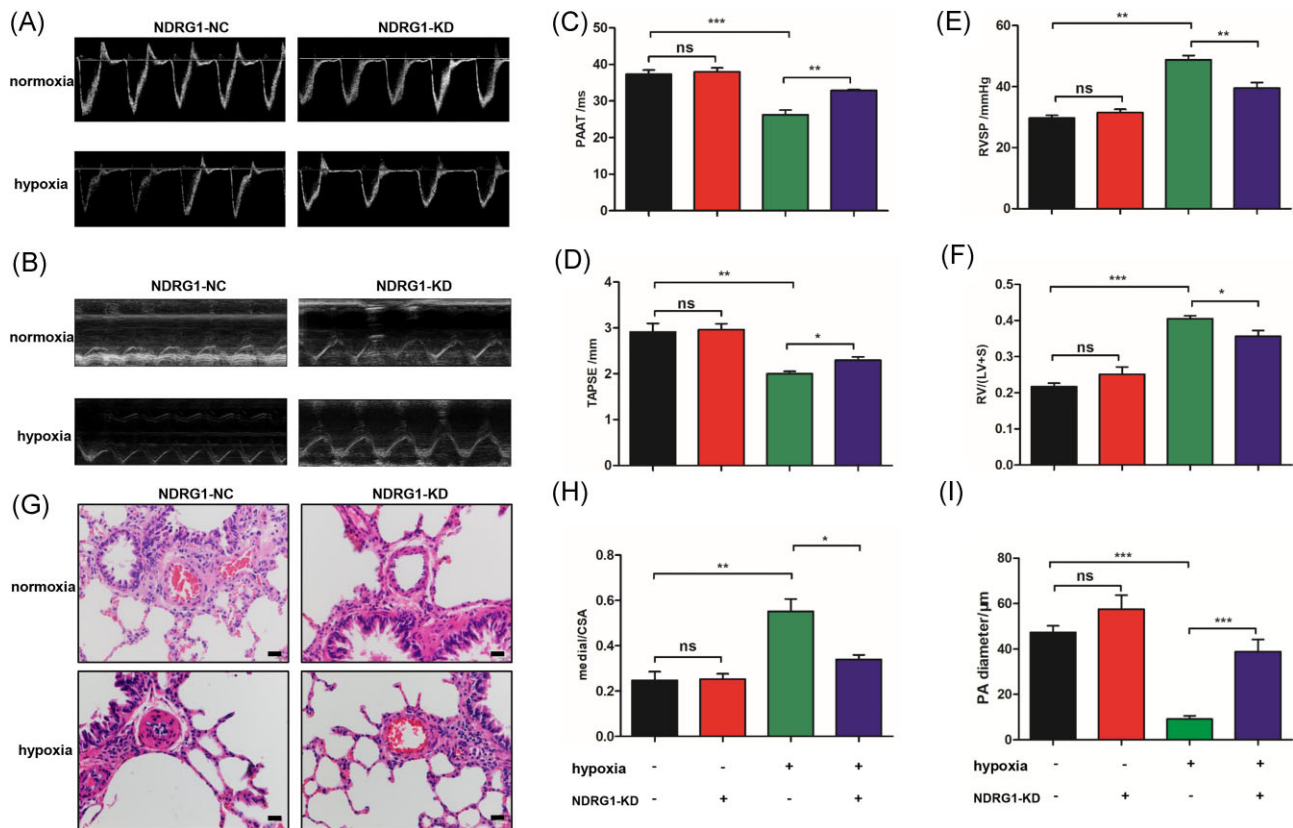


Figure 7. Knockdown of NDRG1 attenuates vascular remodeling and right ventricular hypertrophy in rat. Echocardiography was carried out on rats and PAAT (A,C) and TAPSE (B,D) of the rats were monitored and plotted ($n = 5$). The RVSP (E) and RV/(LV + S) (F) were calculated. (G) H&E staining of paraffin-fixed lung sections prepared from rats for the morphological analysis of pulmonary arteries (scale bar, 20 μm), followed by calculation of the ratio of medial area to cross sectional area (medial/CSA) (H) as well as the diameter of pulmonary arteries (PA) (I). The data are expressed as the means \pm SEMs. * $P < 0.05$, ** $P < 0.01$, *** $P < 0.001$; ns, not significant.

of HIF-1 α under hypoxic conditions.³⁹ Previous research found that digoxin could attenuate hypoxia-induced increases in mean pulmonary arterial pressure and right ventricular hypertrophy compared with those of the hypoxic mice/rats.^{40,41} This phenomenon can be explained by the function of NDRG1 we observed *in vivo* to some extent, however, digoxin downregulates NDRG1 mainly through the inhibition of HIF-1 α , hence, more precise targeting of NDRG1 may be a promising intervention in HPH.

Notably, our IP assay and mass spectrometry analysis indicated that TAF15 is a new binding protein of NDRG1, and immunofluorescence results showed that NDRG1 co-localized with TAF15 in the nucleus of HPAECs. TAF15 is a member of the ten-eleven translocation (TET) family of RNA-binding proteins, and previous studies have found that TAF15 showed both cytoplasmic and nuclear expression in almost all human tissues.⁴² We found here that NDRG1 regulates the subcellular localization of TAF15 in HPAECs. The mechanism by which NDRG1 assists TAF15 in nuclear translocation has not been elucidated. Zhang *et al.* reported that NDRG1 was highly upregulated by Kaposi's sarcoma-associated herpes virus in the nuclei of ECs, forming a complex as a scaffold protein.⁴³ Another study showed that the DNA-binding domain (DBD) of orphan Nur77 (nuclear receptor) was responsible for the binding of NDRG1, and then functionally inhibited the transcriptional activity of Nur77.⁴⁴ Previous investigations also identified the arginine and glycine rich (RGG) domains of TAF15 as responsible for the subcellular localisation or shuttle between the nucleus and the

cytoplasm, which is required for the ability of TAF15 to regulate the expression of endogenous TAF15-target genes.⁴⁵ Further investigation is warranted to determine whether NDRG1 promotes nuclear accumulation of TAF15 through direct interaction with the RGG domain in HPAECs.

As a transcription factor and a component of RNA polymerase II, TAF15 licenses the transcription of a large cohort of genes. Hence, we conducted RNA-seq assay to detect genes affected by TAF15 knockdown in HPAECs. GO analysis confirmed that TAF15 participated in cell migration, angiogenesis, and proliferation. Consistent with this, we found that silencing of TAF15 restored the increased proliferation, migration, and tube formation caused by overexpression of NDRG1. Notably, pathway enrichment assays showed significant associations with key regulatory pathways in PH, including PI3K-Akt, p53, and HIF-1 signaling pathways. PI3K/Akt signaling is one of the most extensively studied signaling pathways fundamental to most biological processes,⁴⁶ regulating cell survival and cell invasion.⁴⁷ Inflammation contributes to the pathogenesis of PH, and our previous study found that crosstalk between the Akt/mTORC1 and nuclear factor kappa-B (NF- κ B) signaling pathways promotes hypoxia-induced PH by increasing dipeptidyl peptidase-4 (DPP4) expression in PSMCs.²⁵ PI3K/Akt signaling is the most typical pathway to regulate endothelial nitric oxide synthase (eNOS) phosphorylation, and the activation of PI3K/AKT/eNOS pathway is important to nitric oxide (NO) production and EC proliferation.^{48,49} Tumor suppressor p53 is a transcription factor that mediates downstream gene regulation of bone morphogenetic protein type 2 receptor (BMP2) in ECs, and

BMPR2–p53 axes are dysregulated in association with endothelial dysfunction in PH.^{50,51} In addition, restoration of p53 signaling in the pulmonary vasculature prevents experimental PH.^{52,53} Cells protect against the consequences of hypoxia by expressing genes that conserve cellular homeostasis, and the most important transcription factors driving these genes are the HIFs. Previous studies demonstrated that HIF-1 contributed to the vascular remodeling response and PH, and provided an appealing candidate mediator of HPH.^{54,55} Interestingly, NDRG1 could be transcriptionally activated by HIF-1 α , indicating that HIF-1/NDRG1/TAF15 may form a closed loop and vicious circle under hypoxia.

In summary, our work demonstrated that endothelial aberrant expression of NDRG1 is a common pathological feature of HPH and is critically involved in endothelial dysfunction through nuclear localization of TAF15, which is further transcriptionally involved in regulating PI3K-Akt, p53, and HIF-1 signaling pathways. NDRG1 also positively functioned in PH development in response to chronic hypoxia in normal animals. Although further studies are needed, these findings undoubtedly provide a new determinant pathological factor and a promising therapeutic target for HPH.

Acknowledgements

This study was supported by the National Natural Science Foundation of China (Grants No. 81970048 and 82270058), starting fund for scientific research of Huashan Hospital Fudan University (Grant No. 2017QD078).

Supplementary data

Supplementary data is available at [PCMED](#) online.

Ethical approval

The study was approved by the local ethical committee (KY2016-396) and written informed consent was obtained from all patients to donate lung tissues. All applicable international, national, and/or institutional guidelines for the care and use of animals were followed.

Conflict of interest

The authors disclose no conflicts of interest.

References

- Ruopp NF, Cockrill BA. Diagnosis and treatment of pulmonary arterial hypertension: A review. *JAMA* 2022;**327**:1379–91. doi:10.1001/jama.2022.4402.
- Humbert M, Kovacs G, Hoeper MM, et al. 2022 ESC/ERS guidelines for the diagnosis and treatment of pulmonary hypertension. *Eur Respir J* 2022;**61**:1–144. doi: 10.1093/eurheartj/ehac237.
- Galiè N, Humbert M, Vachiery JL, et al. 2015 ESC/ERS Guidelines for the diagnosis and treatment of pulmonary hypertension: The Joint Task Force for the Diagnosis and Treatment of Pulmonary Hypertension of the European Society of Cardiology (ESC) and the European Respiratory Society (ERS); endorsed by: Association for European Paediatric and Congenital Cardiology (AEPC), International Society for Heart and Lung Transplantation (ISHLT). *Eur Heart J* 2016;**37**:67–119. doi:10.1093/eurheartj/ehv317.
- Olschewski H, Behr J, Bremer H, et al. Pulmonary hypertension due to lung diseases: updated recommendations from the Cologne Consensus Conference. *Int J Cardiol* 2018;**272s**:63–8. doi:10.1016/j.ijcard.2018.08.043.
- Klinger JR. Group III Pulmonary hypertension: Pulmonary hypertension associated with lung disease: epidemiology, pathophysiology, and treatments. *Cardiol Clin* 2016;**34**:413–33. doi:10.1016/j.ccl.2016.04.003.
- Heresi GA, Platt DM. Healthcare burden of pulmonary hypertension owing to lung disease and/or hypoxia. *BMC Pulm Med* 2017;**17**:58. doi:10.1186/s12890-017-0399-1.
- Chebib N, Mornex JF, Traclet J, et al. Pulmonary hypertension in chronic lung diseases: comparison to other pulmonary hypertension groups. *Pulm Circ* 2018;**8**:2045894018775056. doi:10.1177/2045894018775056.
- Rowan SC, Keane MP, Gaine S, et al. Hypoxic pulmonary hypertension in chronic lung diseases: novel vasoconstrictor pathways. *Lancet Respir Med* 2016;**4**:225–36. doi:10.1016/S2213-2600(15)00517-2.
- Hoeper MM, McLaughlin VV, Dalaan AM, et al. Treatment of pulmonary hypertension. *Lancet Respir Med* 2016;**4**:323–36. doi:10.1016/S2213-2600(15)00542-1.
- Shimoda LA, Laurie SS. Vascular remodeling in pulmonary hypertension. *J Mol Med* 2013;**91**:297–309. doi:10.1007/s00109-013-0998-0.
- Thenappan T, Ormiston ML, Ryan JJ, Archer SL. Pulmonary arterial hypertension: pathogenesis and clinical management. *BMJ* 2018;**360**:j5492. doi:10.1136/bmj.j5492.
- Stenmark KR, Fagan KA, Frid MG. Hypoxia-induced pulmonary vascular remodeling: cellular and molecular mechanisms. *Circ Res* 2006;**99**:675–91. doi:10.1161/01.RES.0000243584.45145.3f.
- Huertas A, Guignabert C. Pulmonary vascular endothelium: the orchestra conductor in respiratory diseases: highlights from basic research to therapy. *Eur Respir J* 2018;**51**:1–13.
- Ranchoux B, Harvey LD, Ayon RJ, et al. Endothelial dysfunction in pulmonary arterial hypertension: an evolving landscape (2017 Grover Conference Series). *Pulm Circ* 2018;**8**:2045893217752912. doi:10.1177/2045893217752912.
- Kurakula K, Smolders V, Tura-Ceide O, et al. Endothelial dysfunction in pulmonary hypertension: cause or consequence? *Biomedicines* 2021;**9**:57. doi:10.3390/biomedicines9010057.
- Evans CE, Cober ND, Dai Z, et al. Endothelial cells in the pathogenesis of pulmonary arterial hypertension. *Eur Respir J* 2021;**58**:2003957. doi:10.1183/13993003.03957-2020.
- Tu L, Dewachter L, Gore B, et al. Autocrine fibroblast growth factor-2 signaling contributes to altered endothelial phenotype in pulmonary hypertension. *Am J Respir Cell Mol Biol* 2011;**45**:311–22. doi:10.1165/rcmb.2010-0317OC.
- Ma C, Li Y, Ma J, et al. Key role of 15-lipoxygenase/15-hydroxyeicosatetraenoic acid in pulmonary vascular remodeling and vascular angiogenesis associated with hypoxic pulmonary hypertension. *Hypertension* 2011;**58**:679–88. doi:10.1161/HYPERTENSIONAHA.111.171561.
- Deng L, Blanco FJ, Stevens H, et al. MicroRNA-143 activation regulates smooth muscle and endothelial cell crosstalk in pulmonary arterial hypertension. *Circ Res* 2015;**117**:870–83. doi:10.1161/CIRCRESAHA.115.306806.
- Ma Z, Yu YR, Badea CT, et al. Vascular endothelial growth factor receptor 3 regulates endothelial function through β -arrestin 1. *Circulation* 2019;**139**:1629–42. doi:10.1161/CIRCULATIONAHA.118.034961.

21. Deshwal H, Weinstein T, Sulica R. Advances in the management of pulmonary arterial hypertension. *J Investig Med* 2021;**69**:1270–80. doi:10.1136/jim-2021-002027.
22. Fang BA, Kovačević Ž, Park KC, et al. Molecular functions of the iron-regulated metastasis suppressor, NDRG1, and its potential as a molecular target for cancer therapy. *Biochim Biophys Acta* 2014;**1845**:1–19. doi:10.1016/j.bbcan.2013.11.002.
23. Park KC, Paluncic J, Kovacevic Z, Richardson DR. Pharmacological targeting and the diverse functions of the metastasis suppressor, NDRG1, in cancer. *Free Radical Biol Med* 2020;**157**:154–75. doi:10.1016/j.freeradbiomed.2019.05.020.
24. Lachat P, Shaw P, Gebhard S, et al. Expression of NDRG1, a differentiation-related gene, in human tissues. *Histochem Cell Biol* 2002;**118**:399–408. doi:10.1007/s00418-002-0460-9.
25. Li Y, Yang L, Dong L, et al. Crosstalk between the akt/mTORC1 and NF- κ b signaling pathways promotes hypoxia-induced pulmonary hypertension by increasing DPP4 expression in PASCs. *Acta Pharmacol Sin* 2019;**40**:1322–33. doi:10.1038/s41401-019-0272-2.
26. Dong L, Liu X, Wu B, et al. Mxi1-0 Promotes hypoxic pulmonary hypertension via ERK/c-myc-dependent proliferation of arterial smooth muscle cells. *Front Genet* 2022;**13**:810157. doi:10.3389/fgene.2022.810157.
27. Costello CM, Howell K, Cahill E, et al. Lung-selective gene responses to alveolar hypoxia: potential role for the bone morphogenetic antagonist gremlin in pulmonary hypertension. *Am J Physiol Lung Cell Mol Physiol* 2008;**295**:L272–284. doi:10.1152/ajplung.00358.2007.
28. Hemnes AR. Using omics to understand and treat pulmonary vascular disease. *Front Med* 2018;**5**:157. doi:10.3389/fmed.2018.00157.
29. Wang Q, Li LH, Gao GD, et al. HIF-1 α up-regulates NDRG1 expression through binding to NDRG1 promoter, leading to proliferation of lung cancer A549 cells. *Mol Biol Rep* 2013;**40**:3723–9. doi:10.1007/s11033-012-2448-4.
30. Koh MY, Powis G. Passing the baton: the HIF switch. *Trends Biochem Sci* 2012;**37**:364–72. doi:10.1016/j.tibs.2012.06.004.
31. Grigoryev DN, Ma SF, Shimoda LA, et al. Exon-based mapping of microarray probes: recovering differential gene expression signal in underpowered hypoxia experiment. *Mol Cell Probes* 2007;**21**:134–9. doi:10.1016/j.mcp.2006.09.002.
32. Hu CJ, Laux A, Gandjeva A, et al. The effect of hypoxia-inducible factor inhibition on the phenotype of fibroblasts in Human and bovine pulmonary hypertension. *Am J Respir Cell Mol Biol* 2023;**69**:73–86. doi:10.1165/rcmb.2022-0114OC.
33. Byun JW, An HY, Yeom SD, et al. NDRG1 and FOXO1 regulate endothelial cell proliferation in infantile haemangioma. *Exp Dermatol* 2018;**27**:690–3. doi:10.1111/exd.13541.
34. Zhang G, Qin Q, Zhang C, et al. NDRG1 signaling is essential for endothelial inflammation and vascular remodeling. *Circ Res* 2023;**132** (3): 306–19. doi: 10.1161/CIRCRESAHA.122.321837.
35. Toffoli S, Delaive E, Dieu M, et al. NDRG1 and CRK-I/II are regulators of endothelial cell migration under Intermittent hypoxia. *Angiogenesis* 2009;**12**:339–54. doi:10.1007/s10456-009-9156-2.
36. Watari K, Shibata T, Fujita H, et al. NDRG1 activates VEGF-A-induced angiogenesis through PLC γ 1/ERK signaling in mouse vascular endothelial cells. *Comm Biol* 2020;**3**:107. doi:10.1038/s42003-020-0829-0.
37. Liu Y, Luo Y, Shi X, et al. Role of KLF4/NDRG1/DRP1 axis in hypoxia-induced pulmonary hypertension. *Biochim Biophys Acta Mol Basis Dis* 2023;**1869**:166794. doi:10.1016/j.bbadis.2023.166794.
38. Chen S, Wei X, Zhang X, et al. Supplementation with Tex261 provides a possible preventive treatment for hypoxic pulmonary artery hypertension. *Front Pharmacol* 2022;**13**:1028058. doi:10.3389/fphar.2022.1028058.
39. Wei D, Peng JJ, Gao H, et al. Digoxin downregulates NDRG1 and VEGF through the inhibition of HIF-1 α under hypoxic conditions in human lung adenocarcinoma A549 cells. *Int J Mol Sci* 2013;**14**:7273–85. doi:10.3390/ijms14047273.
40. Abud EM, Maylor J, Udem C, et al. Digoxin inhibits development of hypoxic pulmonary hypertension in mice. *Proc Natl Acad Sci USA* 2012;**109**:1239–44. doi:10.1073/pnas.1120385109.
41. Yan G, Hu S, Wang Q, et al. Effects of early digoxin treatment on hypoxia-induced pulmonary artery hypertension. (Article in Chinese). *Zhonghua Yi Xue Za Zhi* 2014;**94**:139–43.
42. Andersson MK, Ståhlberg A, Arvidsson Y, et al. The multifunctional FUS, EWS and TAF15 proto-oncoproteins show cell type-specific expression patterns and involvement in cell spreading and stress response. *BMC Cell Biol* 2008;**9**:37. doi:10.1186/1471-2121-9-37.
43. Zhang F, Liang D, Lin X, et al. NDRG1 facilitates the replication and persistence of Kaposi's sarcoma-associated herpesvirus by interacting with the DNA polymerase clamp PCNA. *PLoS Pathog* 2019;**15**:e1007628. doi:10.1371/journal.ppat.1007628.
44. Zhang G, Qin Q, Zhang C, et al. NDRG1 Signaling is essential for endothelial inflammation and vascular remodeling. *Circ Res* 2023;**132**:306–19. doi:10.1161/CIRCRESAHA.122.321837.
45. Jobert L, Argentinini M, Tora L. PRMT1 mediated methylation of TAF15 is required for its positive gene regulatory function. *Exp Cell Res* 2009;**315**:1273–86. doi:10.1016/j.yexcr.2008.12.008.
46. Fruman DA, Chiu H, Hopkins BD, et al. The PI3K pathway in Human disease. *Cell* 2017;**170**:605–35. doi:10.1016/j.cell.2017.07.029.
47. Fruman DA, Rommel C. PI3K and cancer: lessons, challenges and opportunities. *Nat Rev Drug Discov* 2014;**13**:140–56. doi:10.1038/nrd4204.
48. Sabater AL, Andreu EJ, García-Guzmán M, et al. Combined PI3K/Akt and Smad2 activation promotes corneal endothelial cell proliferation. *Invest Ophthalmol Vis Sci* 2017;**58**:745–54. doi:10.1167/iovs.16-20817.
49. Ahmad KA, Ze H, Chen J, et al. The protective effects of a novel synthetic β -elemene derivative on human umbilical vein endothelial cells against oxidative stress-induced injury: involvement of antioxidation and PI3k/Akt/eNOS/NO signaling pathways. *Biomed Pharmacother* 2018;**106**:1734–41. doi:10.1016/j.biopha.2018.07.107.
50. Diebold I, Hennigs JK, Miyagawa K, et al. BMPR2 preserves mitochondrial function and DNA during reoxygenation to promote endothelial cell survival and reverse pulmonary hypertension. *Cell Metab* 2015;**21**:596–608. doi:10.1016/j.cmet.2015.03.010.
51. Hennigs JK, Cao A, Li CG, et al. PPAR γ -p53-mediated vasculoregenerative program to reverse pulmonary hypertension. *Circ Res* 2021;**128**:401–18. doi:10.1161/CIRCRESAHA.119.316339.
52. Mouraret N, Marcos E, Abid S, et al. Activation of lung p53 by Nutlin-3a prevents and reverses experimental pulmonary hypertension. *Circulation* 2013;**127**:1664–76. doi:10.1161/CIRCULATIONAHA.113.002434.
53. Zheng Q, Lu W, Yan H, et al. Established pulmonary hypertension in rats was reversed by a combination of a HIF-2 α antagonist and a p53 agonist. *Br J Pharmacol* 2022;**179**:1065–81. doi:10.1111/bph.15696.

54. Shimoda LA, Manalo DJ, Sham JS, et al. Partial HIF-1alpha deficiency impairs pulmonary arterial myocyte electrophysiological responses to hypoxia. *Am J Physiol Lung Cell Mol Physiol* 2001;**281**:L202–208. doi:10.1152/ajplung.2001.281.1.L202.
55. Frump AL, Selej M, Wood JA, et al. Hypoxia upregulates estrogen receptor β in pulmonary artery endothelial cells in a HIF-1 α -dependent manner. *Am J Respir Cell Mol Biol* 2018;**59**:114–26. doi:10.1165/rcmb.2017-0167OC.